

## Supplementary Information

### Supplementary Materials and Methods

#### Primary Neuronal Culture

All animal experiments were approved by the Animal Experiments Committee at the University of Science and Technology of China (USTCACUC152101034). Low-density co-cultures of dissociated hippocampal neurons and glial cells from E18 rat embryos were prepared as previously described [1]. Glass coverslips (Assistant, Sondheim, Germany) were pre-coated with patterns of poly-L-lysine (PLL) spots of ~1-mm diameter using custom-made stamps [2] or evenly pre-coated with PLL and then covered with ~200  $\mu\text{m}$  thick membranes with 1-mm diameter holes made of polydimethylsiloxane (PDMS, Sylgard 184; Dow Corning, Midland, USA) according to standard soft photolithographic procedures (Fig. S1). Each PLL spot or PDMS hole supported the growth of 50 to 100 neurons mixed with glial cells underneath. Most cultures used in this study were between 12 and 18 days *in vitro* when the neurons formed interconnected networks and evoked reverberatory activity was frequently recorded at this stage. The cultured neuronal networks contained around 10%–20% GABAergic neurons. In some networks that appeared to be dominated by inhibition, doses of bicuculline methiodide (BMI, 0.5–8  $\mu\text{mol/L}$ ) were added to the bath solution to facilitate network activation (Fig. S5). Among all the 29 reverberatory networks tested, 19 exhibited stable evoked reverberation in the absence of bicuculline; 7 exhibited reverberations with a relatively low occurrence, and we added bicuculline to increase the occurrence probability and duration of the evoked reverberation; only 2 networks were non-reverberating at the beginning and became reverberatory after application of  $<2$   $\mu\text{mol/L}$  bicuculline.

#### Electrophysiology

Perforated whole-cell recordings were made using patch-clamp amplifiers (MultiClamp 700A or 700B, Molecular Devices, San Jose, USA) at room temperature. Patch-clamp data were acquired using customized IGOR Pro (WaveMetrics, Portland, USA) programs. Intracellular pipette solution (pH 7.3) contained (in mmol/L): 136.5 potassium gluconate, 17.5 KCl, 9 NaCl, 1 MgCl<sub>2</sub>, 10 HEPES, 0.2 EGTA, and ~200 g/mL amphotericin B. The external bath solution (pH 7.3) contained (in mmol/L): 150 NaCl, 3 KCl, 3 CaCl<sub>2</sub>, 2 MgCl<sub>2</sub>, 10 HEPES, and 5 glucose. Stock solutions of 10 mmol/L BMI were prepared in water and used after dilution in the external bath solution.

### **Ca<sup>2+</sup> Imaging**

Cells were loaded with the membrane-permeable Ca<sup>2+</sup> indicators Fluo-8 AM (TEFLabs, Austin, USA) for 15 min at room temperature. The stock solution of the indicator was prepared to a concentration of 1 or 2 mmol/L in DMSO and stored at -20°C. Before the experiments, it was mixed 1:1 with 20% pluronic F-127 (Invitrogen, Waltham, USA), maintained at room temperature, and diluted in a bath solution at a ratio of 1:1000. Ca<sup>2+</sup> imaging of network activity was performed on an inverted microscope (Olympus IX71, Tokyo, Japan) with a 20× (NA 0.7) objective. Image series were acquired with a Neo sCMOS camera (Andor, Belfast, UK) at a frame rate of 200 Hz. The camera and the light source were both synchronized with electrophysiological stimulation *via* a custom-built hardware triggering circuit. After an experiment, high K<sup>+</sup> solution (same as the intracellular solution but without amphotericin B) was perfused to activate all neurons in the network and obtain high-brightness fluorescence images of all neurons. These images served as high-contrast templates for segmentation in further image analysis.

Differences in imaging time among all pixels in each imaging frame caused by the asynchrony of the rolling shutter during high-speed acquisition were compensated in post-imaging processing procedures.

### **Image Processing**

The fluorescence image series were processed offline using ImageJ and custom MATLAB (MathWorks, Natick, USA) programs. Due to the relatively high spiking rates (5–15 Hz) during reverberation, neuronal  $\text{Ca}^{2+}$  signals responded to each spike increase in a stepwise fashion (Fig. S2A–C), since  $\text{Ca}^{2+}$  clearance was relatively slow (with a time-constant of a few hundred milliseconds). Therefore, the temporal pattern of neuronal firing cannot be directly deduced based on individual  $\text{Ca}^{2+}$  transients, as in cases with lower activity rates [3]. However, changes in fluorescence intensity between adjacent image frames can reflect actual neuronal activation, as long as the image frame rate is faster than the spiking rate of individual neurons during reverberation. Raw fluorescent image series were processed by sequential image subtraction using ImageJ to obtain differential  $\text{Ca}^{2+}$  signals. Bright pixels in a differential image indicate a fast increase in intracellular  $\text{Ca}^{2+}$  and thus reflect neuronal activation. For visualization, the 32-bit differentiated images were further processed by built-in 2D Gaussian blurring in ImageJ. The maximum intensity projection of any given segment of the differential image series produced an image of all neurons activated during the corresponding period.

Neuronal activation was quantified using custom MATLAB programs. Based on the fluorescence intensity  $F(t)$  of each segmented neuron for any given time  $t$  (unit: frame interval), the following variables were calculated:

$$\text{Background } \text{Ca}^{2+} \text{ fluorescence } F_0 = \text{Average}\{F_{\text{background}}\},$$

$$\text{Background-subtracted } \text{Ca}^{2+} \text{ fluorescence } \Delta F = F(t) - F_0,$$

Differential  $\text{Ca}^{2+}$  fluorescence  $\delta F(t) = F(t) - F(t - h)$ , where  $h$  is the number of interleaved frames,

$$\text{Differential } \text{Ca}^{2+} \text{ signals } I(t) = \delta F(t)/F_0,$$

$$\text{Normalized neuronal activation index } I_{\text{norm}}(t) = I(t)/\text{stdev}\{I_{\text{background}}\},$$

Where  $\{F_{\text{background}}\}$  and  $\{I_{\text{background}}\}$  are the sets of  $F$  and  $I$  during the silent period 100 ms

before stimulation, and  $stdev$  is a function for calculating the SD. Peak values of  $I_{norm}$  indicate the statistical significance of putative neuronal spikes against intrinsic noise (Fig. 1E).

## Spike Inference

The high neuronal firing rates and slow  $Ca^{2+}$  clearance caused the nonlinear accumulation of  $Ca^{2+}$  signals, as stated above. We adopted and modified a template-matching-based method for inferring neuronal spikes from  $Ca^{2+}$  fluorescence signals [3].

First, the frames at which each neuron fired were detected by thresholding the differential  $Ca^{2+}$  fluorescence traces. Empirically, only events that passed both the amplitude threshold (5 times SD of the baseline noise) and duration threshold [4 frames for  $\delta_4 F(t)$  traces] were considered to be spiking events. The frames before the detected spiking events were the approximate starter frame of each spike.

A local window of  $\pm 50$  ms ( $\pm 10$  frames) around the starter frames was then fitted. The left part of the window (from  $-50$  ms to  $0$  ms) was simplified as a passive decay of  $Ca^{2+}$ -binding and fitted with a single-exponential decay function:

$$g(t) = A_1 e^{-(t-t_{in})/\tau},$$

$A_1$  and  $\tau$  are fitting variables while  $t_{in}$  is the time fixed as the initial time point of the fitting data (fluorescence at  $t = -50$  ms). Regarding the right part (from  $0$  ms to  $+50$  ms) of the window as a rapid rise followed by passive decay, the whole window ( $\pm 50$  ms) was fitted with the following function:

$$f(t) = \begin{cases} A_2 \left(1 - e^{-\frac{t-t_0}{\tau_{on}}}\right) e^{-\frac{t-t_0}{\tau_1}} + g(t), & t > t_0 \\ g(t), & t \leq t_0 \end{cases}$$

Where  $A_2$ ,  $\tau_{on}$ ,  $\tau_1$  and  $t_0$  are fitting variables, and  $A_1$  and  $\tau$  were determined.

Considering the 1 ms delay between spike initiation and  $Ca^{2+}$  influx,  $T_0 = (t_0 - 1)$  was

regarded as the detected spike timing.

The validity and accuracy of this method were evaluated with a data set acquired from simultaneous electrophysiological recordings and Ca<sup>2+</sup> fluorescence imaging. Each testing neuron was stimulated at 5–20 Hz under the current-clamp mode (1 ms, 1000 pA). We typically obtained a temporal resolution of  $\pm 2.3$  ms with a 95% confidence region of 4.9 ms (Fig. S2F).

The 200 Hz frame rate allowed resolution of  $<10$  ms, according to the Nyquist sampling theorem. However, what we obtained from fitting was the starting point of each spike-induced fluorescence curve, not the complete information of the source signal. Therefore, it does not violate the Nyquist theorem.

### Pattern Analysis

We used a previously described method [4] to evaluate the similarity between reverberatory event pairs. After spike inference, each spike was temporally convolved with a normalized Gaussian kernel (sigma = 3 ms) to obtain a smooth representation of the local firing probability of a given neuron at the given time point. Individual reverberation events were split and extracted by adding the convolved spiking signals of all neurons and thresholding. The mean value and SD of the firing rate were calculated for all neurons during the reverberatory episode. A candidate event was accepted only if the firing rate exceeded the mean +  $3 \times$  SD and lasted for at least 20 ms. The similarity index (SI) is

$$SI(n, m) = \max \left( \sum_{i=1}^N C_i^{n,m}(\tau) \right),$$

where  $C_i^{n,m}(\tau)$  is the cross-correlation coefficient of the differential spiking signal of neuron  $i$  between event  $n$  and  $m$ , given the same time lag  $\tau$  for all neurons.

Extracted reverberation events were spatially shuffled or temporally jittered and then compared to the original results [5]. Spiking events were shuffled spatially across neurons while their timings remained, or were jittered temporally by a random interval ( $\pm \Delta T$ ) while the neuron order was

unchanged. After shuffling or jittering, the SIs of control events were calculated with the same method. The final SIs were the average of 1000 random shuffling and jittering events. To avoid artifacts introduced by differences in firing frequency among neurons, we only shuffled or jittered neurons that were active during reverberation.

## Supplementary References

- [1] Bi GQ, Poo MM. Synaptic modifications in cultured hippocampal neurons: Dependence on spike timing, synaptic strength, and postsynaptic cell type. *J Neurosci* 1998, 18: 10464–10472.
- [2] Lau PM, Bi GQ. Synaptic mechanisms of persistent reverberatory activity in neuronal networks. *Proc Natl Acad Sci U S A* 2005, 102: 10333–10338.
- [3] Grewe BF, Langer D, Kasper H, Kampa BM, Helmchen F. High-speed *in vivo* Ca<sup>2+</sup> imaging reveals neuronal network activity with near-millisecond precision. *Nat Methods* 2010, 7: 399–405.
- [4] Segev R, Baruchi I, Hulata E, Ben-Jacob E. Hidden neuronal correlations in cultured networks. *Phys Rev Lett* 2004, 92: 118102.
- [5] Ikegaya Y, Aaron G, Cossart R, Aronov D, Lampl I, Ferster D, *et al.* Synfire chains and cortical songs: Temporal modules of cortical activity. *Science* 2004, 304: 559–564.

## Supplementary Movies

**Movie S1** Dynamics of Ca<sup>2+</sup> fluorescence in a reverberatory network. The video shows background-subtracted Fluo-8 fluorescence images from the same network shown in Fig. 1A during the period from –100 to 895 ms in the reverberation episode shown in Fig. 1G. Original images were acquired at 200 frames/s and played back at 10 frames/s (1/20 real-time speed). Background fluorescence (average

Ca<sup>2+</sup> image before the stimulus) was subtracted from all raw images. A stimulus pulse was given to a single patch-clamped neuron at 0 ms, causing its activation and rapid Ca<sup>2+</sup> increase, followed by subsequent activation of other neurons in the network. Raw imaging data were acquired at a pixel resolution of 1200 × 1050 and binned to 600 × 525 here in order to reduce movie size.

**Movie S2** Population neuronal activity in a reverberatory network revealed by differential Ca<sup>2+</sup> imaging. The displayed image series were obtained by calculating changes in pixel intensity of adjacent frames of the same original image series used in Movie 1. Here, bright pixels indicate changes in Ca<sup>2+</sup> fluorescence, primarily due to neuronal action potential firing. The spatiotemporal dynamics of reverberatory activity are reflected by repeated wave-like bursts of bright flashes traveling through the network. Playback is at 10 frames/s (1/20 real-time speed).

## Supplementary Figures

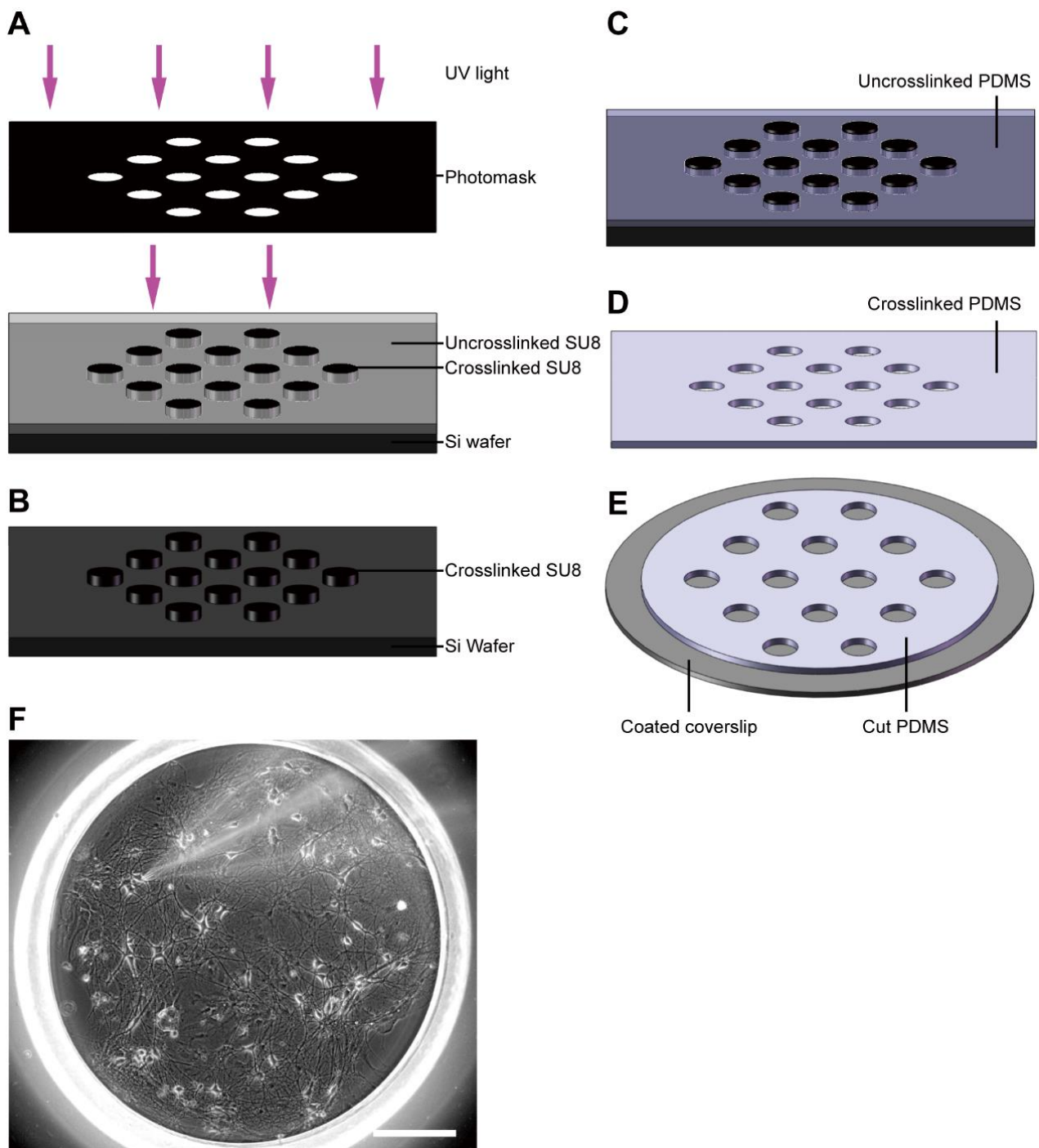


**Fig. S1** Microfabrication of PDMS devices for culturing isolated hippocampal networks. **A–E** Pipeline of photolithography and PDMS molding. **A** Negative photoresist (SU8 2150, Microchem Inc., Westborough, USA) is coated onto a silicon wafer and exposed to UV light passed through a custom-designed photomask (made by Microclear Inc). **B** Crosslinking photoresist on the wafer forms tiny



columns (diameter, 1 mm; height, 250–300 nm). **C** PDMS (mixed at 1:10 ratio, Sylgard 184, Dow Corning) is spin-coated onto the wafer and forms a 150–200 nm thick layer. The wafer is then heated at 80°C for 30 min. **D, E** The heat-crosslinked PDMS membrane is peeled off the wafer, cut, and then attached to glass coverslips coated with poly-L-lysine. **F** An example phase-contrast image of an isolated cultured hippocampal network. Scale bar, 200  $\mu\text{m}$ .

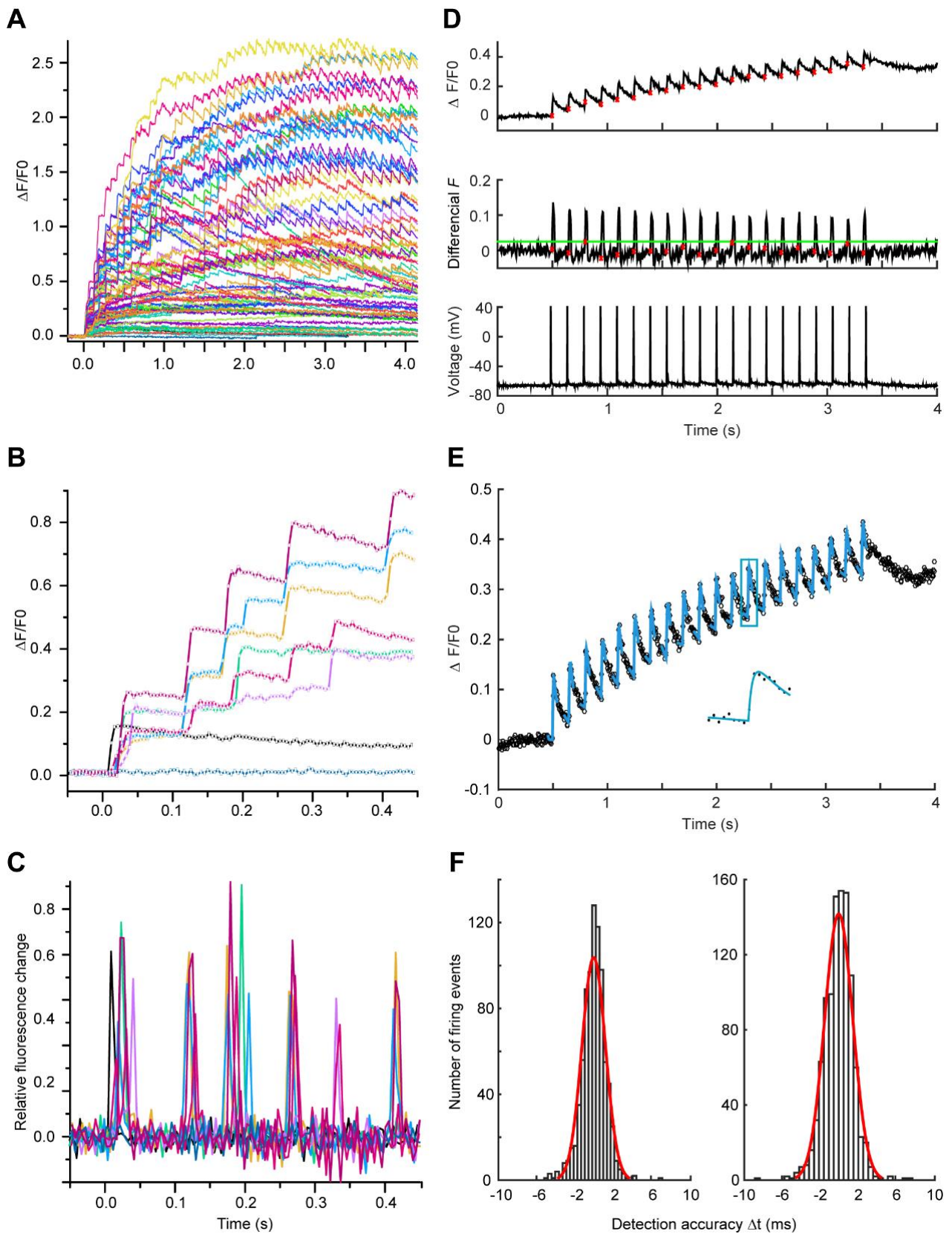


**Fig. S2** Spike inference from step-wise  $\text{Ca}^{2+}$  fluorescence traces. **A**  $\text{Ca}^{2+}$  fluorescence signals of all 69 neurons identified in the network shown in Fig. 1A–E during reverberation (corresponding to trial

number 1 in Fig. 1B). Stimulation was applied at time 0. Each colored trace represents one neuron. **B** Expanded view of the fluorescence signal of 8 representative neurons from those shown in **A**. The black trace is from the stimulated neuron under voltage clamp. **C** Normalized neuronal activation signal calculated using the data set shown in **B**. The same color represents the same neuron for both **B** and **C**. **D** A train of stimuli (voltage traces shown below) induces a step-wise increase of  $\text{Ca}^{2+}$  fluorescence (upper trace), to mimic neuronal firing during reverberatory events. Raw firing timing was measured from the differential ( $n = 4$ ) traces of  $\text{Ca}^{2+}$  fluorescence by thresholding (middle trace). **E** After the raw firing timings were found, local fitting was made to determine more accurate spike timings. Insert: an enlarged view of the boxed area. **F** Summary histograms of the distribution of  $\Delta t$ , the difference between predicted spike time and actual spike time. With different firing frequencies (left: 20 Hz, 826 firing events; right: 6.67 Hz, 1014 firing events), the 95% confidence intervals from Gaussian fits are each 4.92 ms and 5.96 ms.

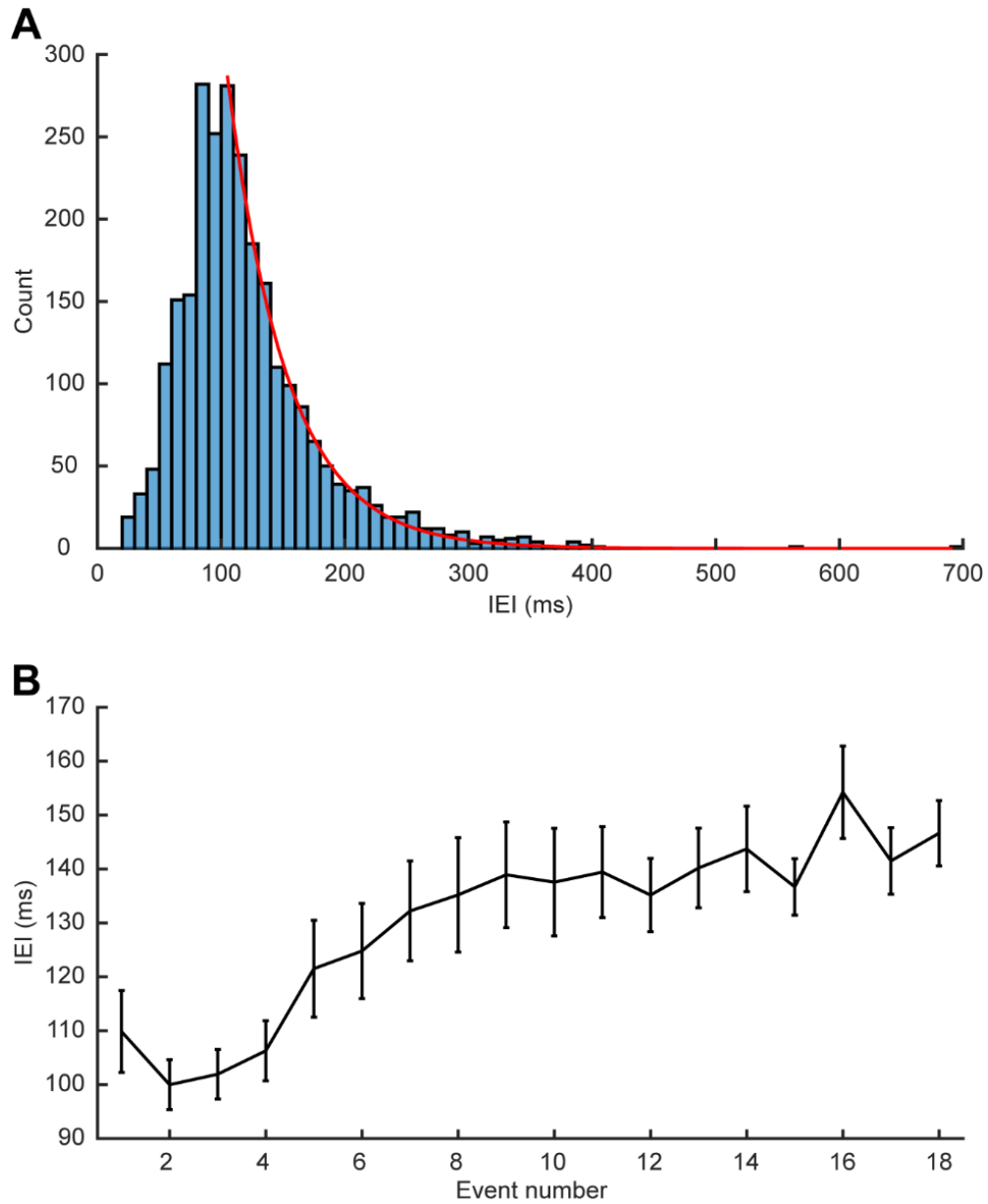


**Fig. S3** Oscillation frequency of reverberatory networks. **A** Distribution of inter-event intervals (IEIs) from 29 recorded reverberatory networks. The average IEI from all the networks is  $121.2 \pm 1.1$  ms. The distribution of IEIs  $>100$  ms was fit to an exponential decay ( $y = A \times e^{-t/\tau}$ ,  $A = 2564$ ,  $\tau = 48.0$ ). **B** The change of IEI during a reverberatory episode. The IEI gradually increases as reverberation progresses. The trace is an average of 29 reverberatory networks. Bars are  $\pm$ SEM.

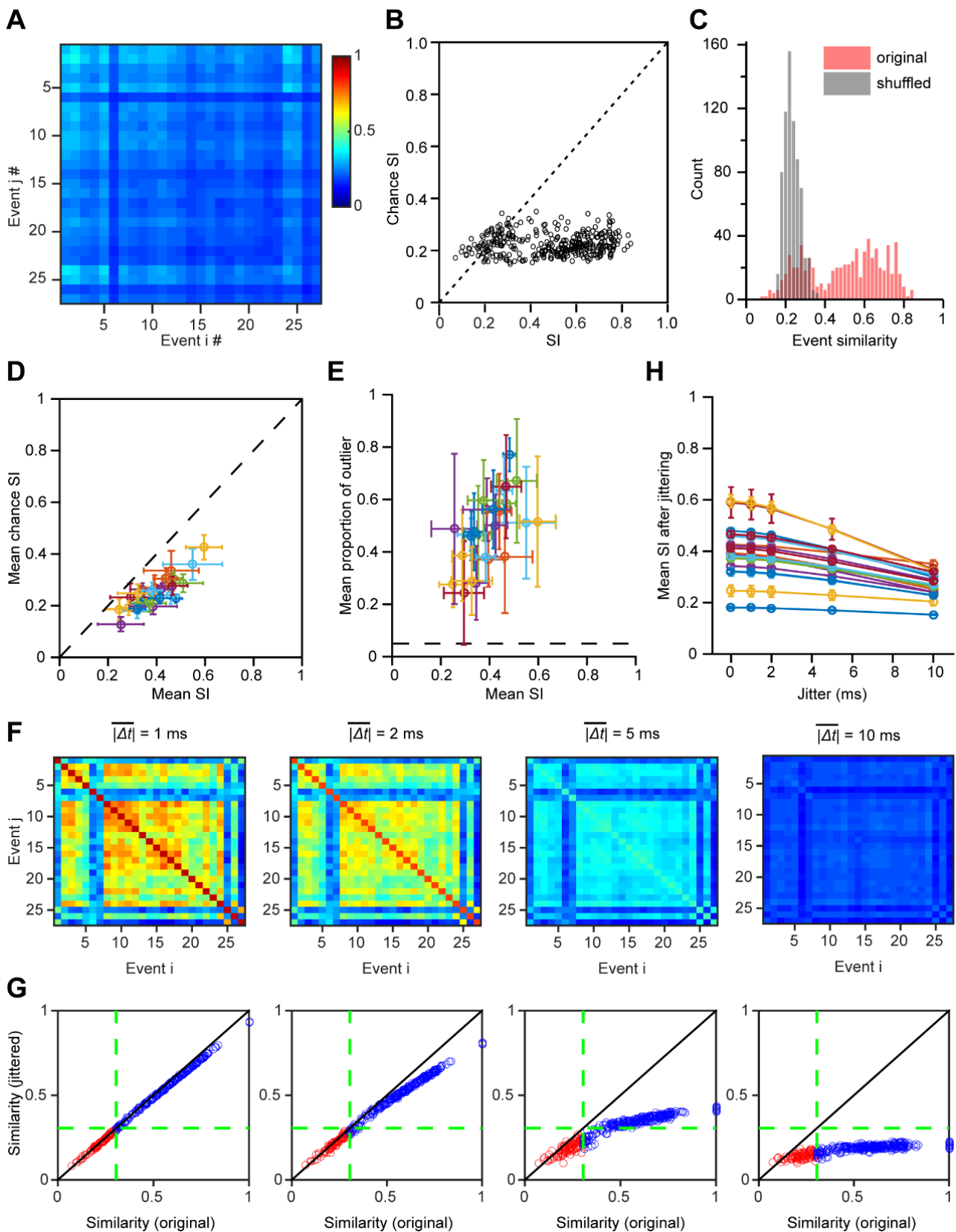


**Fig. S4** Shuffling and jittering of reverberatory events reduces the similarity of event pairs. **A** SIs of the event pairs in Fig. 1H calculated after spike shuffling. **B** Raster plot of event-pair similarity indexes

of original (SI) and shuffled data (random SI). **C** Distribution of event-pair similarity indexes of original and shuffled data. **D** Pattern similarity of all 26 examined networks (in different colors), represented by the mean SI value of all event pairs in reverberatory episodes. **E** Proportion of event pairs in which the SI was significantly larger ( $\text{mean} + 2 \times \text{SD}$ ) than those by chance (evaluated from the shuffling data set) from all 26 examined networks. Error bars denote SDs among multiple network episodes for **D** and **E**. **H** SIs calculated with temporally jittered data with different jitters ( $\overline{|\Delta t|} = 0, 1, 2, 5, \text{ or } 10 \text{ ms}$ ). Error bars are SEM. **F** SIs of event pairs in different temporal jitter intervals. Each spike during an event was jittered randomly from a uniform distribution ranging from  $-t_j$  to  $t_j$  ( $t_j = 2, 4, 10, 20 \text{ ms}$ , thus  $|\Delta t| = 1, 2, 5, 10 \text{ ms}$ ). **G** SIs calculated after jittering compared to the SIs of intact event pairs.

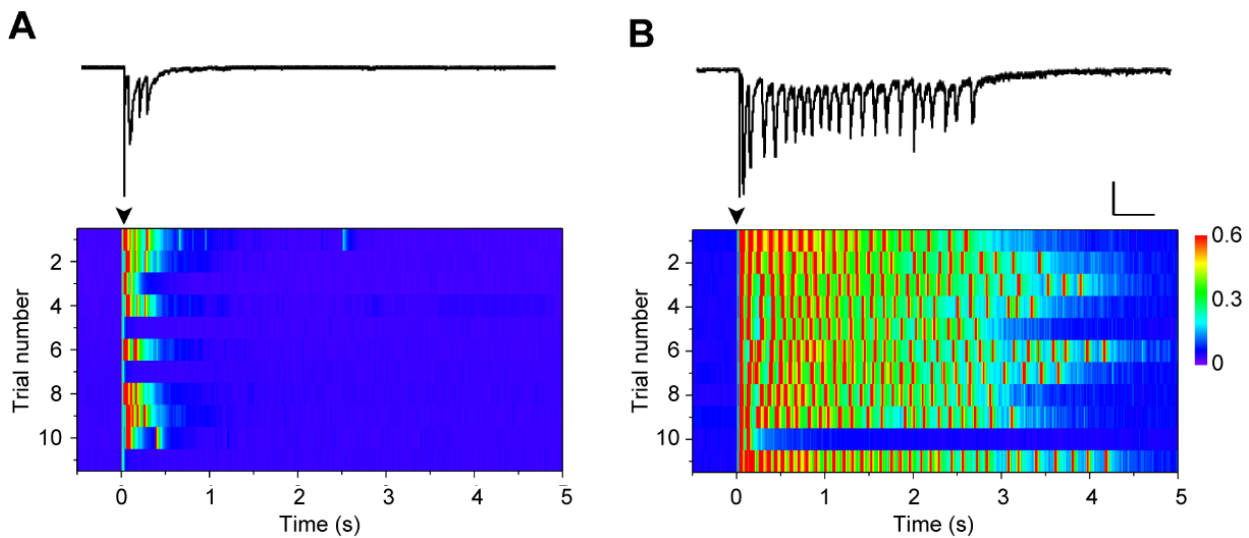


**Fig. S5** Bicuculline facilitates network activation. **A** Short reverberation evoked by single-pulse stimuli. Stimulation pulses were given every 30 s at the time indicated by the arrowhead. Top: polysynaptic current trace recorded from the reverberatory network (trial number 4). **B** 0.5  $\mu\text{mol/L}$  bicuculline increases both the duration and occurrence of reverberation. Scale bars: 0.5 s, 300 pA. Color codes for the amplitude of polysynaptic currents (nA).